

Electronic Supplementary Information (ESI)

Luminescence characteristics of rare-earth-doped barium hexafluorogermanate BaGeF₆ nanowires: fast subnanosecond decay time and high sensitivity in H₂O₂ detection

Gibin George,^a Machael D. Simpson,^a Bhoj R. Gautam,^a Dong Fang,^b Jinfang Peng,^{†c} Jianguo Wen,^c Jason E. Davis,^d Daryush Ila^a and Zhiping Luo ^{*a}

^a *Department of Chemistry and Physics, Fayetteville State University, Fayetteville, NC 28301, USA. E-mail: zluo@uncfsu.edu*

^b *College of Materials Science and Engineering, Kunming University of Science and Technology, Kunming 650093, P. R. China*

^c *Centre for Nanoscale Materials, Argonne National Laboratory, Argonne, Illinois 60439, USA*

^d *Oak Ridge Institute for Science and Education, Oak Ridge Associated Universities, Oak Ridge, TN 37830, USA*

Results

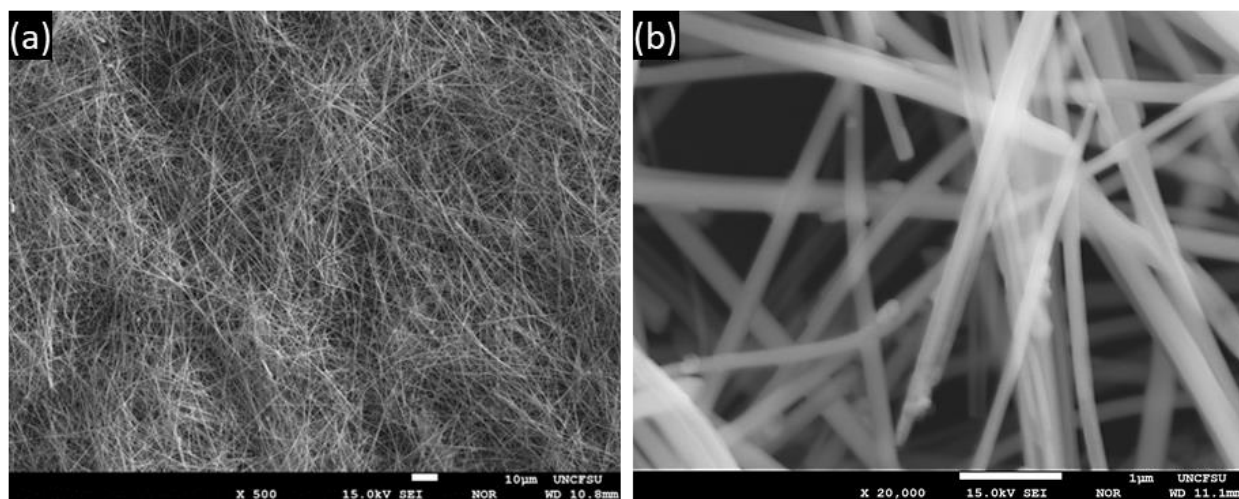


Fig. S1. SEM images of BGF:2Ce nanowire phosphors revealing the high aspect ratio; at (a) low and (b) high magnifications.

[†] Present address: Southwest Jiaotong University, Chengdu 610031, P. R. China.

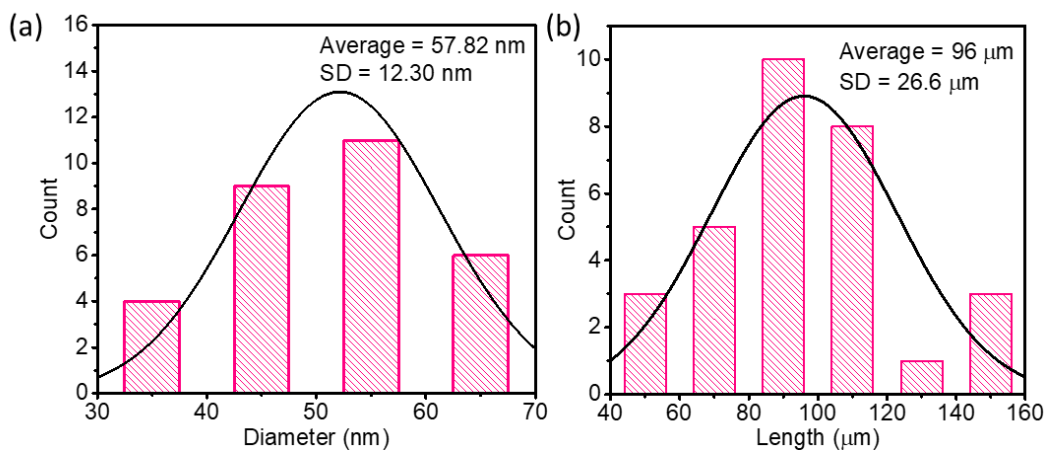


Fig. S2. Diameter and length distribution of 30 nanowires, corresponding average and standard deviation are in the inset.

Table S1. Composition BGF nanowires from EDS analysis.

Elements	Mass %	Atomic %	Nominal Mass %	Nominal Atomic %
Ba	42.5	11.9	42.39	12.50
Ge	19.3	10.3	22.42	12.50
F	38.2	77.8	35.19	75.00

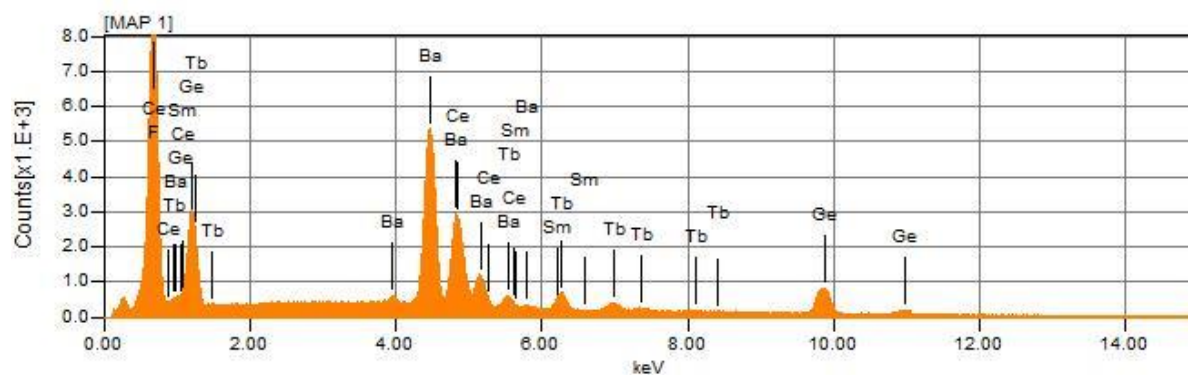


Fig. S3. EDS spectra of BGF: 1Ce-15Tb-0.5Sm nanowire phosphors.

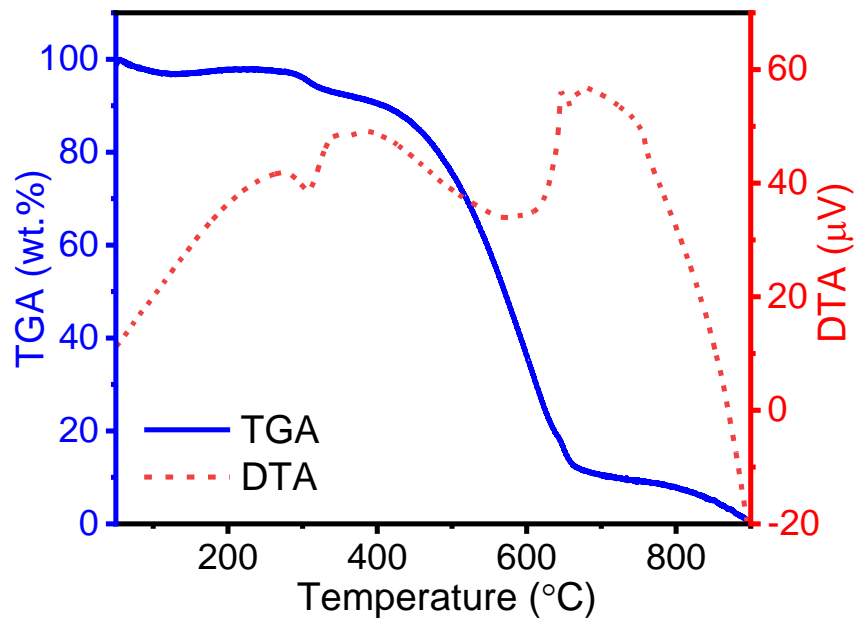


Fig. S4. TG analysis of pure BGF nanowires

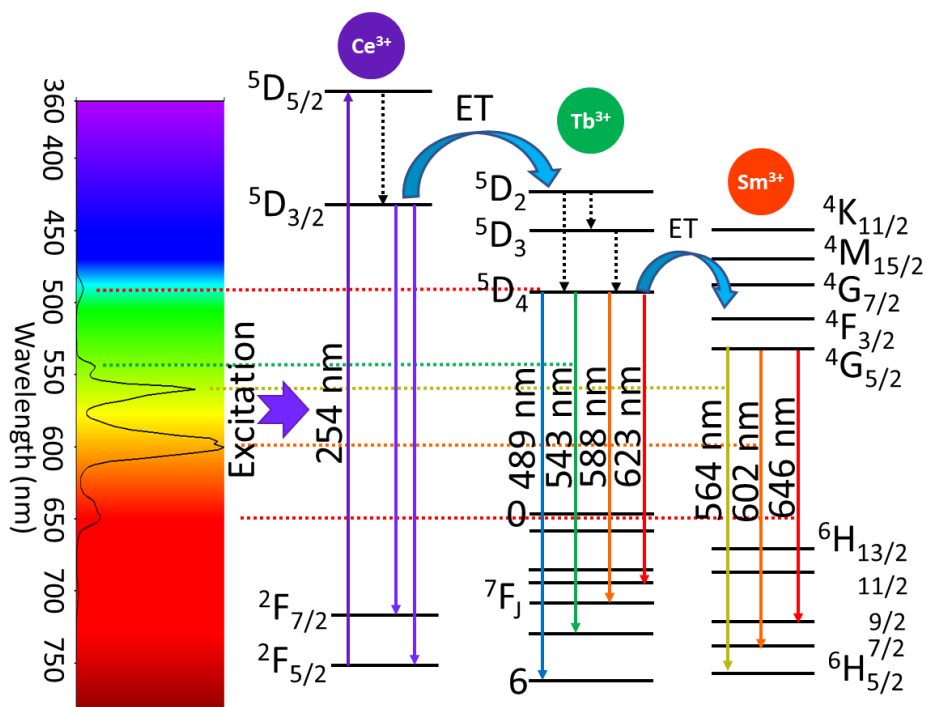


Fig. S5. Mechanism of energy transfer in BGF:*x*Ce-*y*Tb-*z*Sm nanowire phosphors.

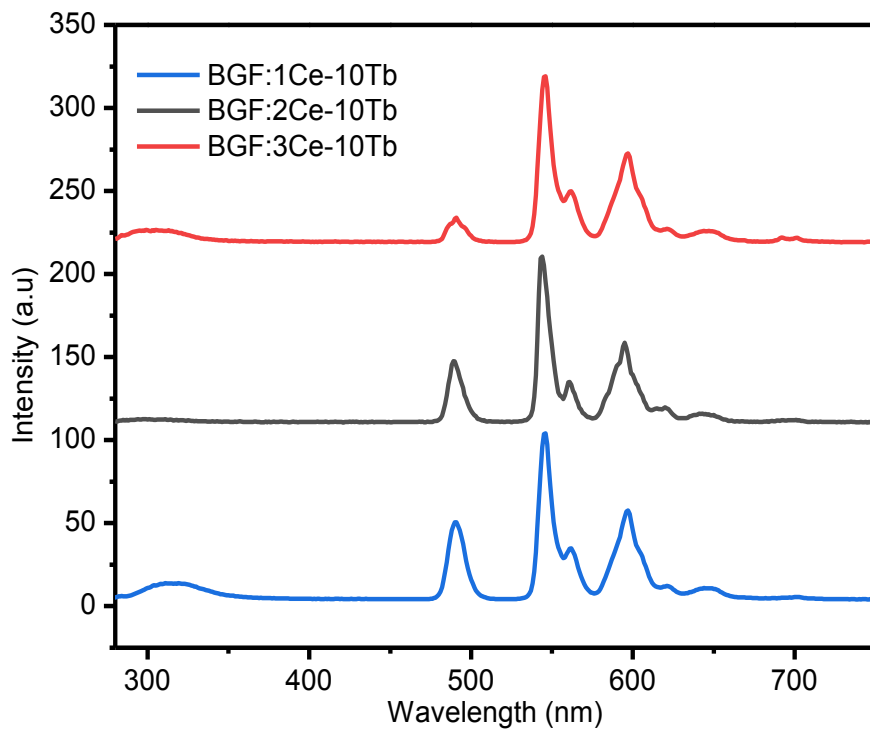


Fig. S6. PL emission from the BGF:xCe-10Tb nanowire phosphors under 254 nm excitation.

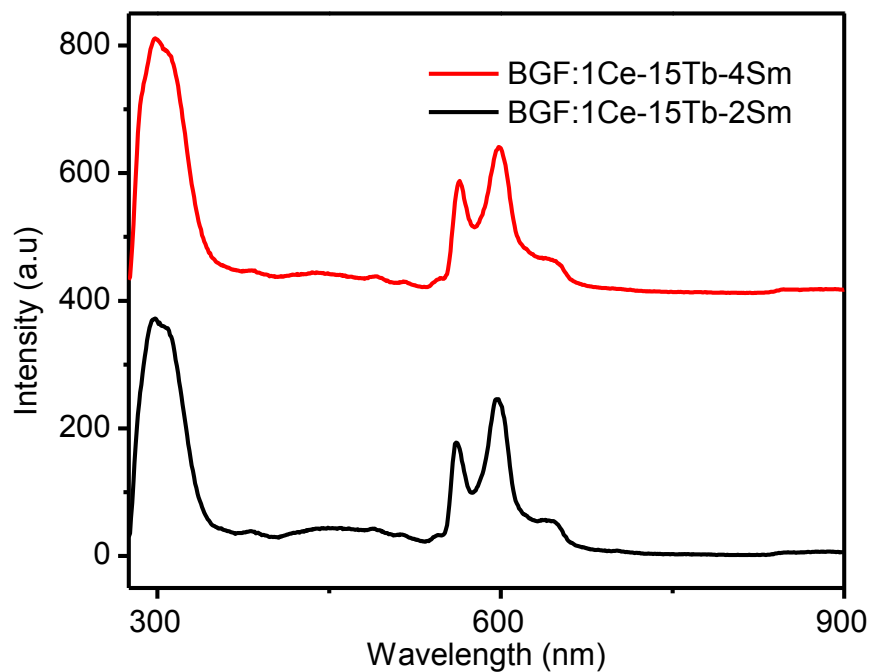


Fig. S7. PL emission from the BGF nanophosphors with high Sm^{3+} doping under 254 nm excitation.

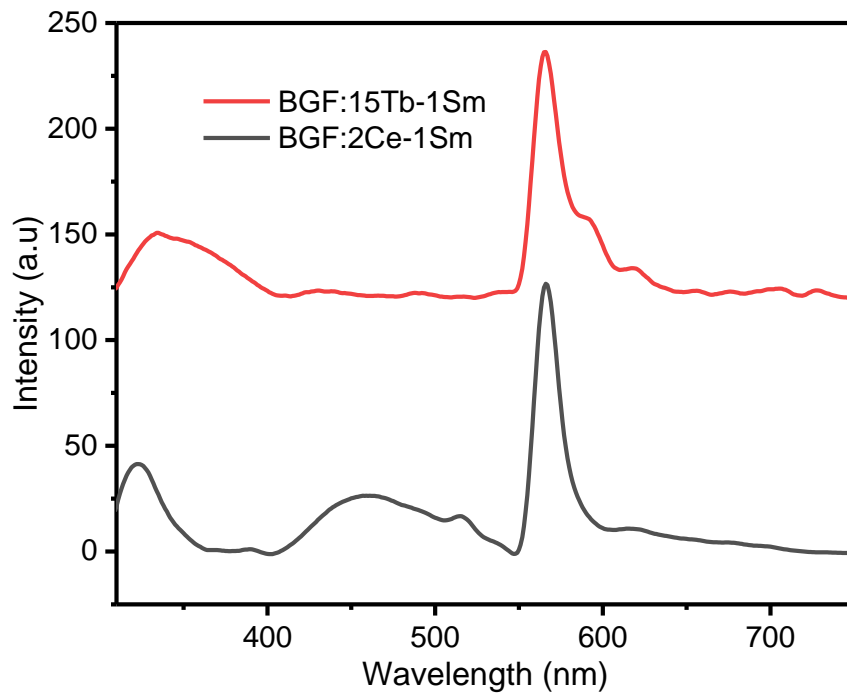


Fig. S8. PL emission from the binary doped BGF nanowire phosphors under 254 nm excitation.

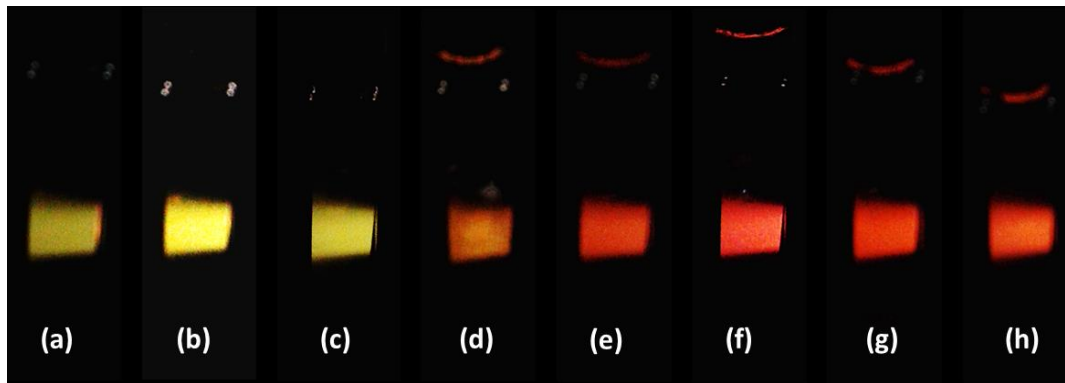


Fig. S9. Photographs of emission from the nanophosphors under 254 nm excitation (a) BGF:1Ce-10Tb, (b) BGF:1Ce-15Tb, (c) BGF:1Ce-30Tb, (d) BGF:1Ce-15Tb-0.01Sm, (e) BGF:1Ce-15Tb-0.02Sm, (f) BGF:1Ce-15Tb-0.05Sm (g) BGF:1Ce-15Tb-0.1Sm, and (d) BGF:1Ce-15Tb-0.5Sm.

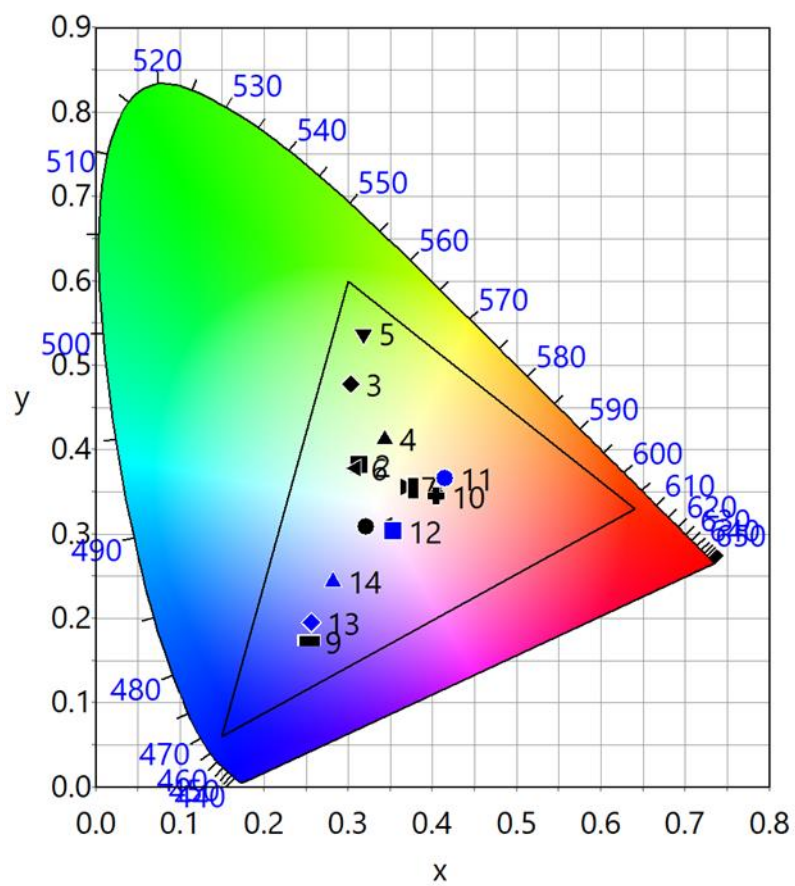


Fig. S10. CIE diagram of codoped BGF nanowire phosphor PL emission.

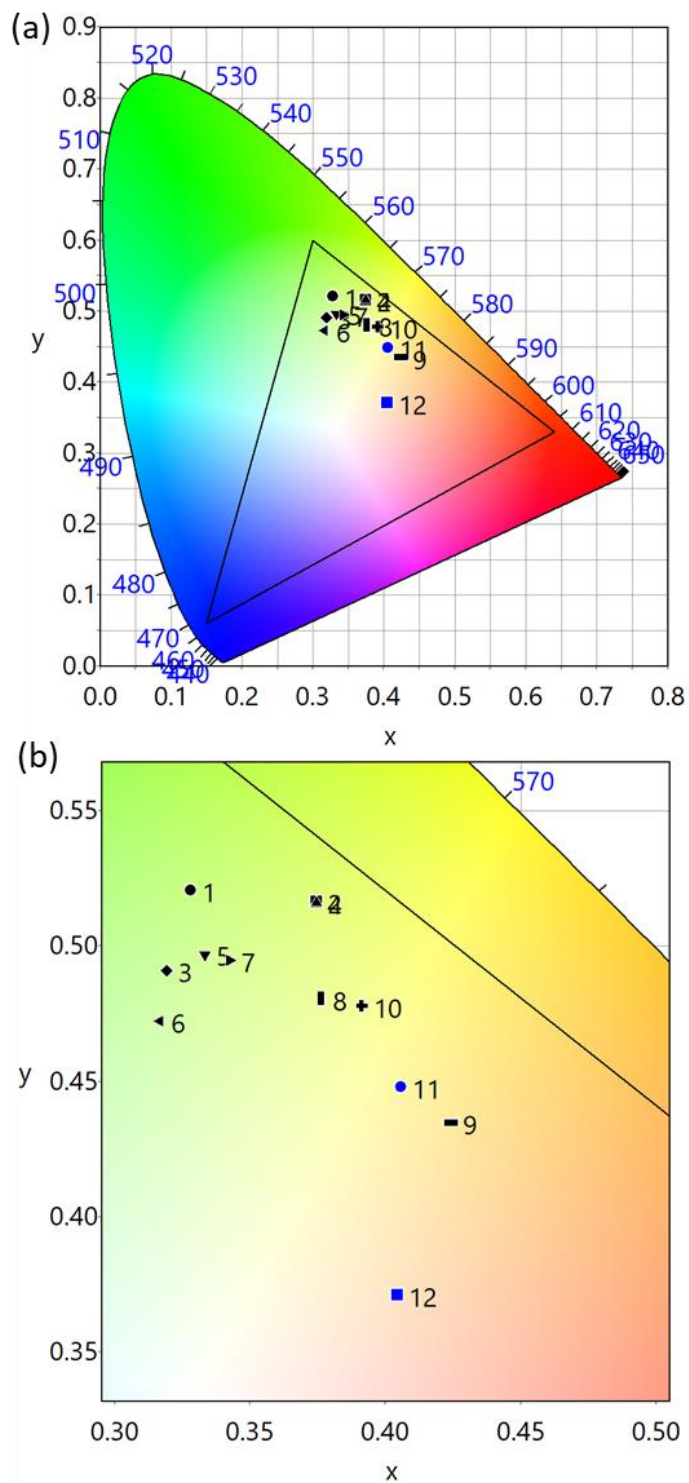


Fig. S11. (a) CIE diagram of BGF:xCe-yTb-zSm nanowire phosphor CL emission, and (b) enlarged view of (a).

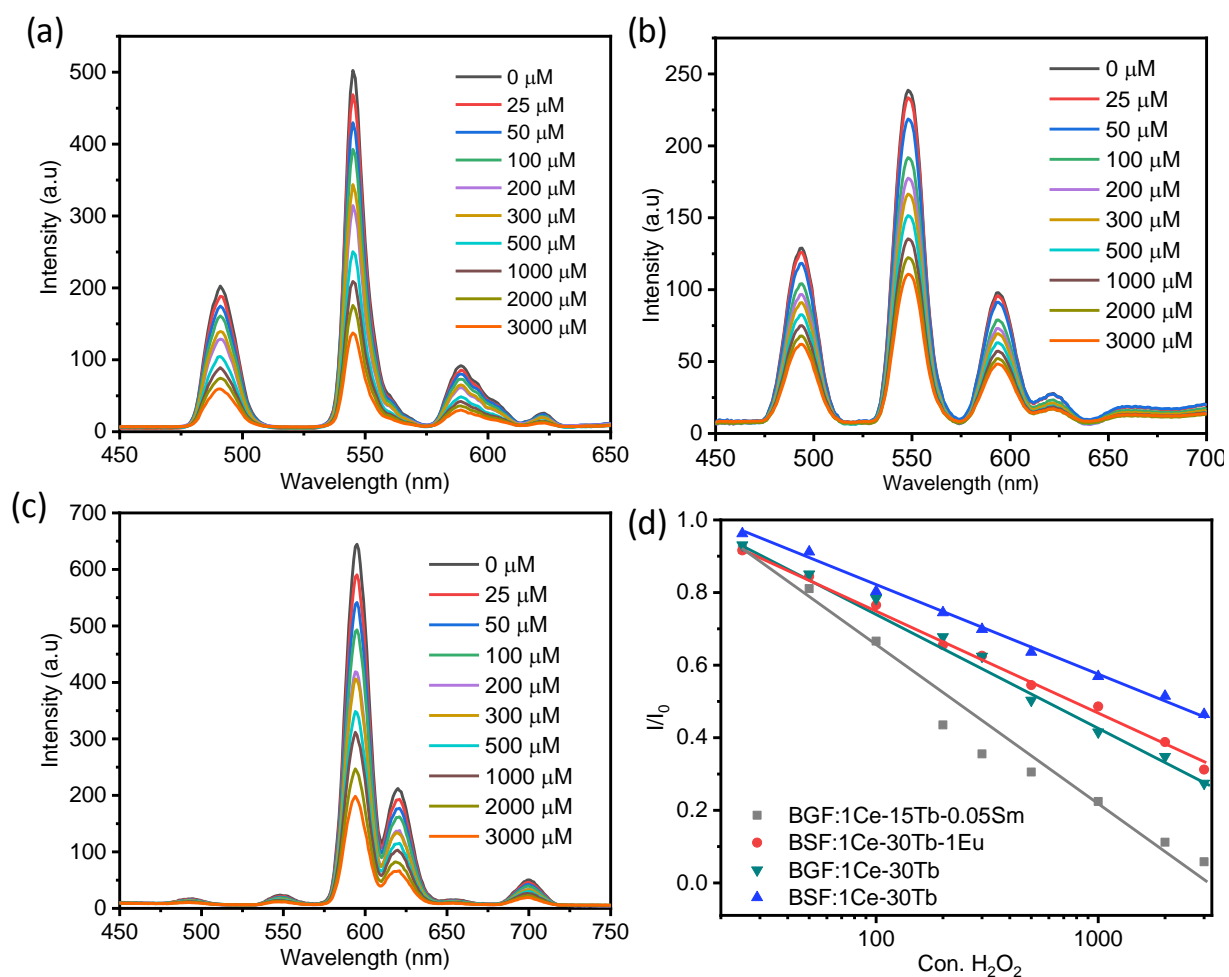


Fig. S12. PL response of nanowires towards H_2O_2 concentration, (a) BaGeF₆ nanowires codoped with 1 mol.% Ce³⁺ and 30 mol.% Tb³⁺, (b) (a) BaSiF₆ nanowires codoped with 1 mol.% Ce³⁺ and 30 mol.% Tb³⁺, (c) (a) BaSiF₆ nanowires codoped with 1 mol.% Ce³⁺, 30 mol.% Tb³⁺, and 1 mol.% Eu³⁺, and (d) comparison of calibration curves.

Table S2. The observed, calculated and residual values of the fit in Fig. 10a inset.

Con. H ₂ O ₂ (μ M)	I/I ₀		Residual values
	Observed	Calculated	
25	0.91892	0.89159	0.02733
50	0.81081	0.76411	0.0467
100	0.66622	0.63662	0.02959
200	0.43514	0.50914	-0.074
300	0.35541	0.43457	-0.07916
500	0.30541	0.34061	-0.03521
1000	0.22432	0.21313	0.01119
2000	0.11216	0.08565	0.02652
3000	0.05811	0.01107	0.04704

Table S3. The observed, calculated and residual values of the fit in Fig. 10b.

Con. H ₂ O ₂ (μ M)	Quenching Efficiency (%)		Residual values
	Observed	Calculated	
25	8.10811	10.84097	-2.73286
50	18.91892	23.58936	-4.67044
100	33.37838	36.33775	-2.95937
200	56.48649	49.08614	7.40035
300	64.45946	56.54347	7.91599
500	69.45946	65.9386	3.52086
1000	77.56757	78.68699	-1.11942
2000	88.78378	91.43538	-2.65159
3000	94.18919	98.89271	-4.70352